Pergamon

Journal of Structural Geology, Vol. 16, No. 5, pp. 663 to 676, 1994

0191-8141/94 $07.00+0.00

Strain partitioning in ductile shear zones: an example from a Lower Pennine nappe of Switzerland

S. MOHANTY* and J. G. RAMSAY

Geologisches Institut, ETH-Zentrum, 8092 Zürich, Switzerland

(*Received* 22 *May* 1990; *accepted in revised form* 25 *June* 1993)

Abstract—The rocks of the Maggia nappe, a Lower Pennine nappe of the Swiss Alps, were deformed in at least three phases during Alpine orogeny. Hercynian granites in the core of the nappe developed ductile shear zones during the early phases of deformation, but between shear zones they remained almost undeformed. Both heterogeneous simple shear and heterogeneous volume change played an important role in the formation of the ductile shear zones. Partitioning of different strain components indicates a volume loss of nearly 80–90% towards the centres of some of the shear zones. Such a large amount of volume loss is also corroborated by strain analysis of deformed xenoliths in other shear zones of the same region. A comparative study of theoretical strain paths and the natural results indicates constant shear strain rate but changing dilation rate during deformation.

INTRODUCTION

IDEAL ductile shear zones develop under any combination of three main types of displacement field: heterogeneous simple shear, heterogeneous volume change and uniform homogeneous strain (Ramsay & Graham 1970, Ramsay 1980). Strain markers, such as deflected planar markers, schistosity, deformed xenoliths and deformed mineral aggregates, can be used to determine the finite strain in shear zones. Mathematically it is possible to make partitioning of this finite strain into its different components (Ramsay & Graham 1970, Ramsay 1980, Ramsay & Huber 1987). In any shear zone analysis, such an attempt might be used to develop a better understanding of physico-chemical processes involved in the development of the shear zone. In this contribution, we will review the methods to derive the finite strain matrix and will demonstrate their application in one of the Lower Pennine nappes of the Swiss Alps.

THE FINITE STRAIN MATRIX FOR DUCTILE SHEAR ZONES

In a two-dimensional, plane strain kinematic framework, with the x-axis parallel to the shear zone boundary, the displacement equations for the three main components of strain in ductile shear zones are as follows.

For simple shear parallel to the walls

$$\begin{bmatrix} x' \\ y' \end{bmatrix} = \begin{bmatrix} 1 & -\gamma \\ 0 & 1 \end{bmatrix} \begin{bmatrix} x \\ y \end{bmatrix}. \tag{1}$$

The negative sign for shear strain (γ), in the equation above, arises by shear convention (left-handed positive and right-handed negative).

For volume change (Δ) across the walls

$$\begin{bmatrix} x' \\ y' \end{bmatrix} = \begin{bmatrix} 1 & 0 \\ 0 & 1+\Delta \end{bmatrix} \begin{bmatrix} x \\ y \end{bmatrix}. \tag{2}$$

For homogeneous strain in the shear zone and its wall rocks

$$\begin{bmatrix} x' \\ y' \end{bmatrix} = \begin{bmatrix} p & q \\ r & s \end{bmatrix} \begin{bmatrix} x \\ y \end{bmatrix}, \tag{3}$$

where p, q, r and s represent the constant terms of the homogeneous strain.

The total final deformation in the shear zone can be derived by multiplying the strain matrices in equations (1), (2) and (3). Since matrix multiplication is non-commutative, the order of multiplication has to be specified. We put these constraints on the system: the displacement conditions with more freedom follow the displacements with less freedom with reference to the movement frame, although all three displacements probably occur together. It is well known that deformation by simple shear parallel to the x-axis is dependent on position along the y-axis and is independent of position along the x-axis. On the other hand, both homogeneous strain and volume change are dependent on the positions along the x-axis as well as on the y-axis. An inspection of the strain matrices in equations (2) and (3) indicates that the strain matrix for volume change (involving coefficients which are usually 0 and 1) is simpler than that for the homogeneous strain. The mathematics are expressed in simplest form ordering the components in the form: (1) homogeneous strain; and (2) volume change. Again, if the condition of deformation is such that the dimension along the x-axis does not change during deformation, the finite volume change will depend on the change in dimension along the y-axis. For these reasons, the strain matrix for volume change should be superposed on that for the homogeneous strain and the resultant should be multiplied by that

*Present address: Department of Applied Geology, Indian School of Mines, Dhanbad 826004, India.

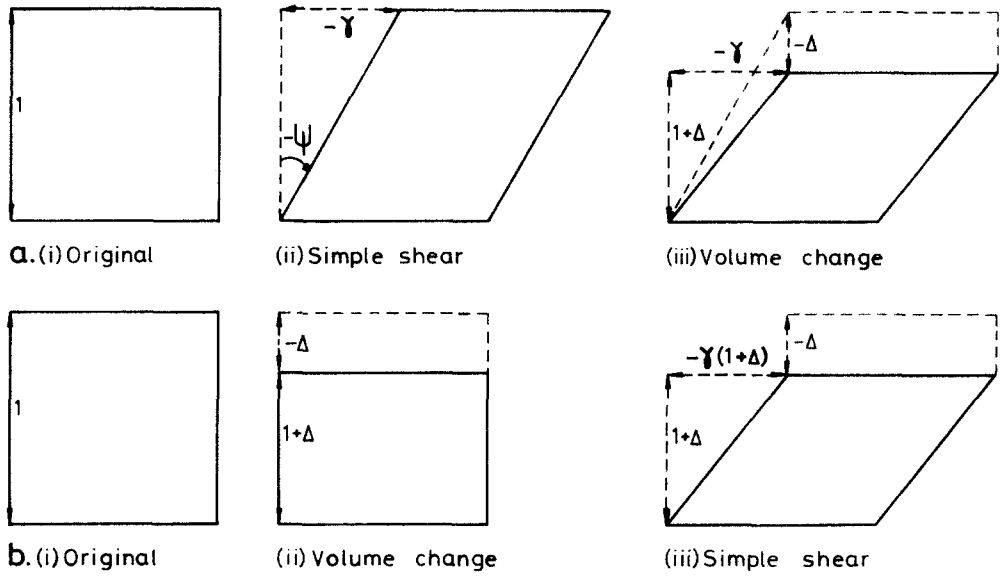

Fig. 1. Geometrical significance of the order of superposition of strain matrices: (a) simple shear followed by volume change, and (b) volume change followed by simple shear.

of the simple shear. The finite strain matrix under such conditions, is given by

$$\begin{matrix}\text{3rd}\\ \begin{bmatrix}1 & -\gamma\\ 0 & 1\end{bmatrix}\end{matrix}\begin{matrix}\text{2nd}\\ \begin{bmatrix}1 & 0\\ 0 & 1+\Delta\end{bmatrix}\end{matrix}\begin{matrix}\text{1st}\\ \begin{bmatrix}p & q\\ q & s\end{bmatrix}\end{matrix}$$

$$= \begin{bmatrix} p - r\gamma(1+\Delta) & q - s\gamma(1+\Delta) \\ r(1+\Delta) & s(1+\Delta) \end{bmatrix}. \quad (4)$$

The matrices in equation (4) are arranged in the order shown above them, following the standard convention that superposition of deformations proceeds from right to left.

Ramsay & Graham (1970) have shown that if the walls of the shear zone are unstrained, only simple shear and volume change can occur in combination, and the strain matrix for homogeneous strain becomes a unit matrix. With such boundary conditions, the finite strain matrix is given by

$$\begin{matrix}\text{2nd}\\ \begin{bmatrix}1 & -\gamma\\ 0 & 1\end{bmatrix}\end{matrix}\begin{matrix}\text{1st}\\ \begin{bmatrix}1 & 0\\ 0 & 1+\Delta\end{bmatrix}\end{matrix} = \begin{bmatrix}1 & -\gamma(1+\Delta)\\ 0 & (1+\Delta)\end{bmatrix}. \quad (5)$$

In equation (5), the strain matrix for simple shear is superposed on that of the volume change, the choice for such an order being explained earlier. The importance of this is illustrated in Fig. 1. If volume loss follows simple shear (Fig. 1a), the angle of shear (ψ) increases further during volume change. The real value of shear strain in this case is greater than the computed result. On the other hand, when volume loss precedes simple shear (Fig. 1b) the real value of the shear strain is the same as the computational value. In both methods, the amount of volume change is the same. Although the mathematics compels us to superpose one strain matrix on the other, it is not implied that one displacement physically takes place after the other has been completed; both processes may, and probably do, take place simultaneously. Summarizing, for a particular final shear angle, method (a) of matrix multiplication gives a lower shear strain value than the actual amount obtained by method (b).

Therefore, for strain partitioning in ductile shear zones, we have to look for mathematical methods to determine the unknown parameters in equations (4) or (5).

USE OF STRAIN MARKERS TO DETERMINE THE STRAIN PARAMETERS OF DUCTILE SHEAR ZONES

Two planar markers

When a planar marker (the trace of a planar structural surface on the profile section of the shear zone) undergoes passive rotation (Fig. 2), its initial orientation (α) before deformation and final orientation (α') after deformation, with respect to the x-axis, are related to each other by the equation

$$\tan\alpha' = \frac{c + d\tan\alpha}{a + b\tan\alpha}, \quad (6)$$

where a, b, c and d are the constant terms of the finite strain matrix (Ramsay & Huber 1983, p. 286).

By substituting the value of the constant terms for the undeformed wall condition, from (5), we have

$$\tan\alpha' = \frac{(1+\Delta)\tan\alpha}{1 - \gamma(1+\Delta)\tan\alpha}. \quad (7)$$

On simplification, we get

$$\cot\alpha' = \frac{\cot\alpha}{(1+\Delta)} - \gamma. \quad (8)$$

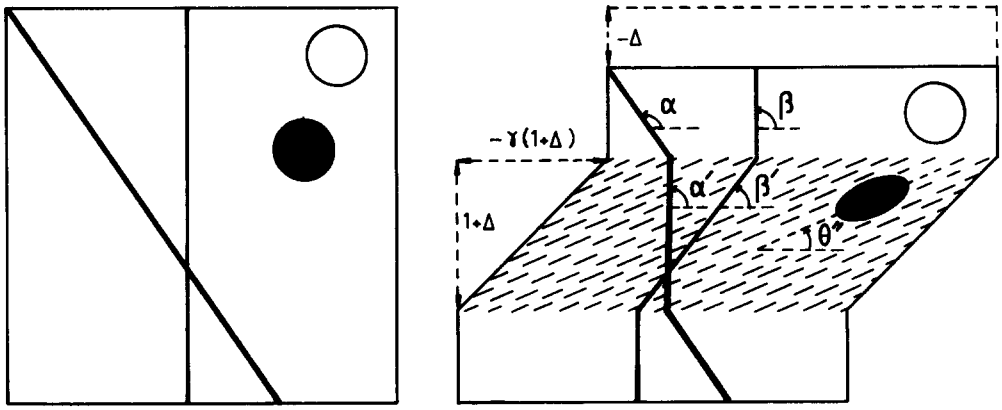

Fig. 2. Geometrical relations between two planar markers, schistosity and the strain ellipse in a shear zone developed by simple shear and volume loss.

Since equation (8) is linear in nature involving two unknowns, γ and $(1 + \Delta)$, we can solve it if we know the orientations of two planar markers inside a shear zone (α' and β') and their orientations outside the shear zone (α and β), with respect to the shear zone walls (Fig. 2). We have

$$\gamma = \frac{\cot\alpha' \cot\beta - \cot\alpha \cot\beta'}{\cot\alpha - \cot\beta} \tag{9}$$

$$1 + \Delta = \frac{\cot\alpha - \cot\beta}{\cot\alpha' - \cot\beta'}. \tag{10}$$

Schistosity and one planar marker

The orientation (θ'') of the long axis of the strain ellipse with respect to the x-axis, in any deformation, is given by the equation

$$\tan 2\theta'' = \frac{2(ac + bd)}{a^2 + b^2 - c^2 - d^2} \tag{11}$$

(Ramsay & Huber 1983, p. 286).

Substituting the values of a, b, c and d, for undeformed walls, we have

$$\tan 2\theta'' = \frac{-2\gamma(1 + \Delta)^2}{1 + \gamma^2 \cdot (1 + \Delta)^2 - (1 + \Delta)^2}. \tag{12}$$

On simplification, we have

$$\gamma^2 + 2\gamma \cot 2\theta'' + \frac{1}{(1 + \Delta)^2} - 1 = 0. \tag{13}$$

Since the value of θ'' can be determined from the orientation of the schistosity with respect to the shear zone boundary (Fig. 2b), equation (13) can be solved if any one of the two unknowns, γ and $(1 + \Delta)$, is known. Thus, if the orientations of any planar marker inside and outside the shear zone are known together with the orientation of the schistosity, then we can substitute the value of $(1 + \Delta)$ from equation (8) in terms of γ, α and α', in equation (13). This on simplification gives the following result:

$$\gamma^2 (1 + \tan^2\alpha) + 2\gamma (\cot\alpha' \tan^2\alpha + \cot 2\theta'') + (\tan^2\alpha \cot^2\alpha') - 1 = 0. \tag{14}$$

This is a quadratic equation in the form

$$A\gamma^2 + B\gamma + C = 0. \tag{15}$$

Hence we will get two values of γ:

$$\gamma = \frac{-B \pm \sqrt{B^2 - 4AC}}{2A}. \tag{16}$$

By substituting these values in equation (8) we can get two values of $(1 + \Delta)$. The problem of selecting the pair of correct solutions is solved knowing that $(1 + \Delta)$ should be always positive and that γ should show signs consistent with the observed shear displacement.

If the wall rocks are also deformed, a similar procedure can be followed to evaluate equations (6) and (11) by substituting the constants from equation (4), but one has to know the ellipticity of the final strain ellipse and the ellipse orientation inside and outside the shear zone, in addition to any of the above two requirements (see Ramsay & Huber 1987, p. 601).

APPLICATION OF THE STRAIN PARTITIONING TECHNIQUE IN A LOWER PENNINE NAPPE OF THE SWISS ALPS

In order to apply the technique of strain partitioning, ductile shear zones in the core of the Maggia nappe, a Lower Pennine nappe of the Swiss Alps (Figs. 3a & b), were mapped in detail. The studied area occurs northeast of Pne. dei Laghetti (Fig. 3c) in Canton Ticino, Switzerland (Topo sheet of Switzerland, No. 265, coordinates 689.25:147.06). The area can be approached by a motorable road connecting Locarno with Lake Naret, via Fusio, with a walk for about 1 h from the parking place near the upper Laghetti lake, through a northwesterly sloping valley and a small pass north of Pne. dei Laghetti (see Fig. 3c). An area of approximately 875 m^2 (Fig. 4), with nearly horizontal, smooth outcrop surface, representing the true profile section of

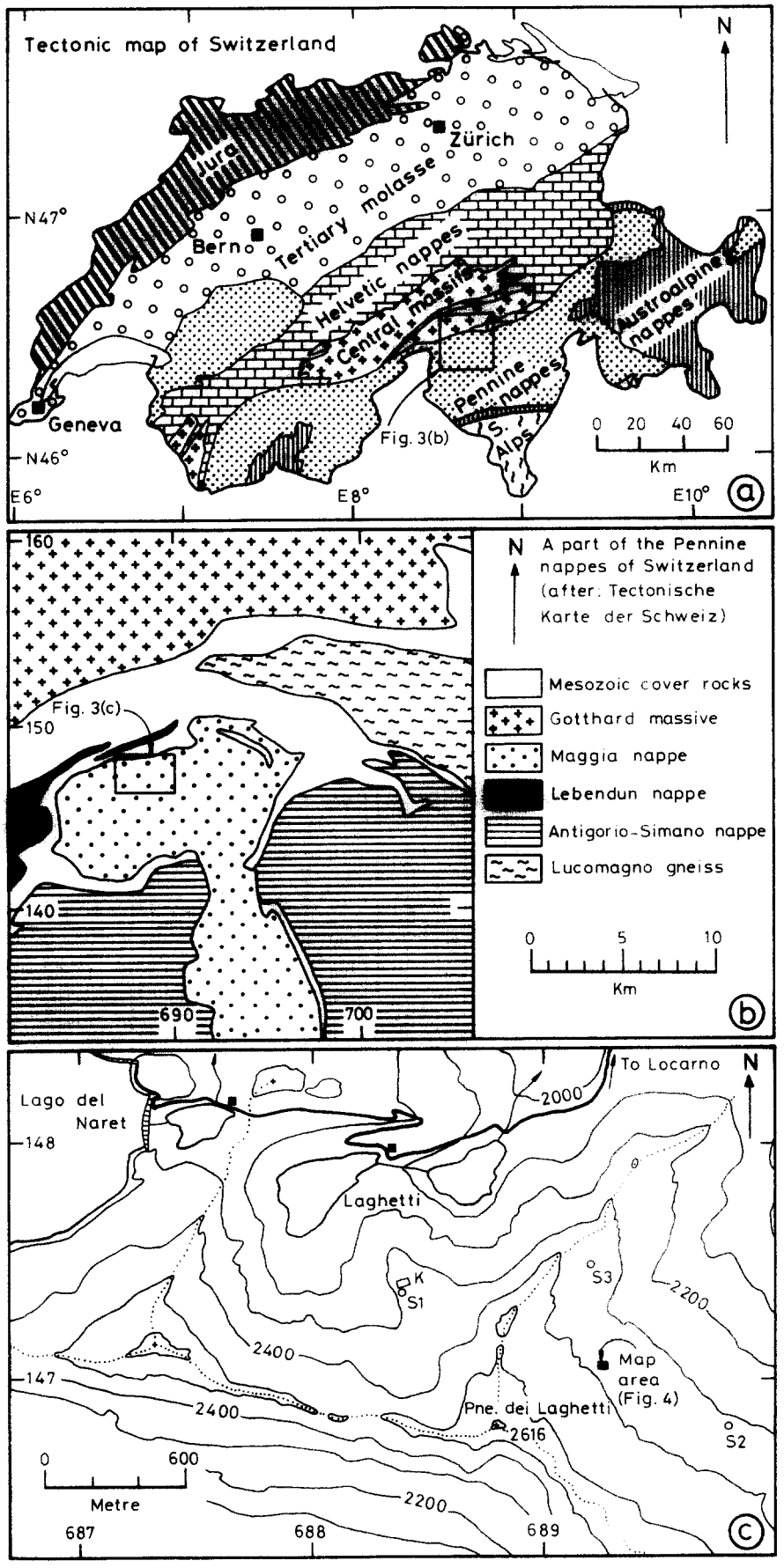

Fig. 3. (a) Tectonic units of Switzerland. (b) Geological setting of the Maggia nappe. (c) Topographic map of the Laghetti area, showing the locations of the mapped area and of samples analysed by previous workers (K = Kerrich *et al.* 1977 and S = Simpson 1981)

the shear zones, was mapped at a scale of 1:25 using a 1 m square grid marked off in 10 cm intervals.

Geological framework of the region

The Maggia nappe contains two main stratigraphic units: pre-Triassic igneous rocks, forming the basement, and Mesozoic metasedimentary cover rocks. The basement rocks forming the core of the nappe comprise intrusions of different ages. The earliest of these are granodiorite, diorite, adamellite and tonalite, followed by homogeneous granite. These early-formed plutonic rocks were subsequently intruded by lamprophyre, and aplite and pegmatite dykes, respectively (Ramsay & Graham 1970, Ramsay & Allison 1979). U–Pb age determinations of zircons in the basement rocks indicate an age of 1600–2500 Ma for detrital grains and 280–340 Ma (Hercynian age) for idiomorphic grains (Köppel *et al.* 1981).

Both the basement and cover rocks were deformed in at least three phases during the Alpine orogeny (Ramsay & Graham 1970, Ayrton & Ramsay 1974, Ramsay & Allison 1979, Huber *et al.* 1980, Ramsay & Huber 1987, pp. 479–480 and 491–493). The first deformation was responsible for large-scale ductile flow and the formation of the main nappe structure. The second deformation led to the refolding of the early formed structures. The third deformation produced the regional back-folding of the whole nappe. The regional metamorphism of the basement and its cover rocks, was syn- to post-tectonic with respect to the second deformation. Biotite–garnet geothermometry and plagioclase–garnet geobarometry by Klaper (1982), indicate metamorphism under amphibolite facies condition, at 560° ± 40°C temperature and 6–7 kbar pressure.

Strain analysis technique and results

Shear zones in homogeneous granite, showing sigmoidal schistosity bounded by rocks showing no fabric, are exposed on subhorizontal surfaces (Figs. 4 and 5). Both right-handed and left-handed shear zones are common in the area. Differently oriented aplite dykes cutting across the granite body show deflection in the shear zones (Fig. 4). Dioritic xenoliths inside the granite body show stretching parallel to the schistosity inside the shear zones, but are practically undeformed in the wall rocks (Fig. 5). Although many dykes are deflected inside shear zones, some are non-planar in nature. Therefore, three planar dykes in the northwestern part of the area (see Fig. 4 for location) were chosen for final analysis. In this location the shear zone boundary shows slight curvature. Such boundary deflections are explained by propagation under plane strain condition (Ramsay 1980, p. 94,

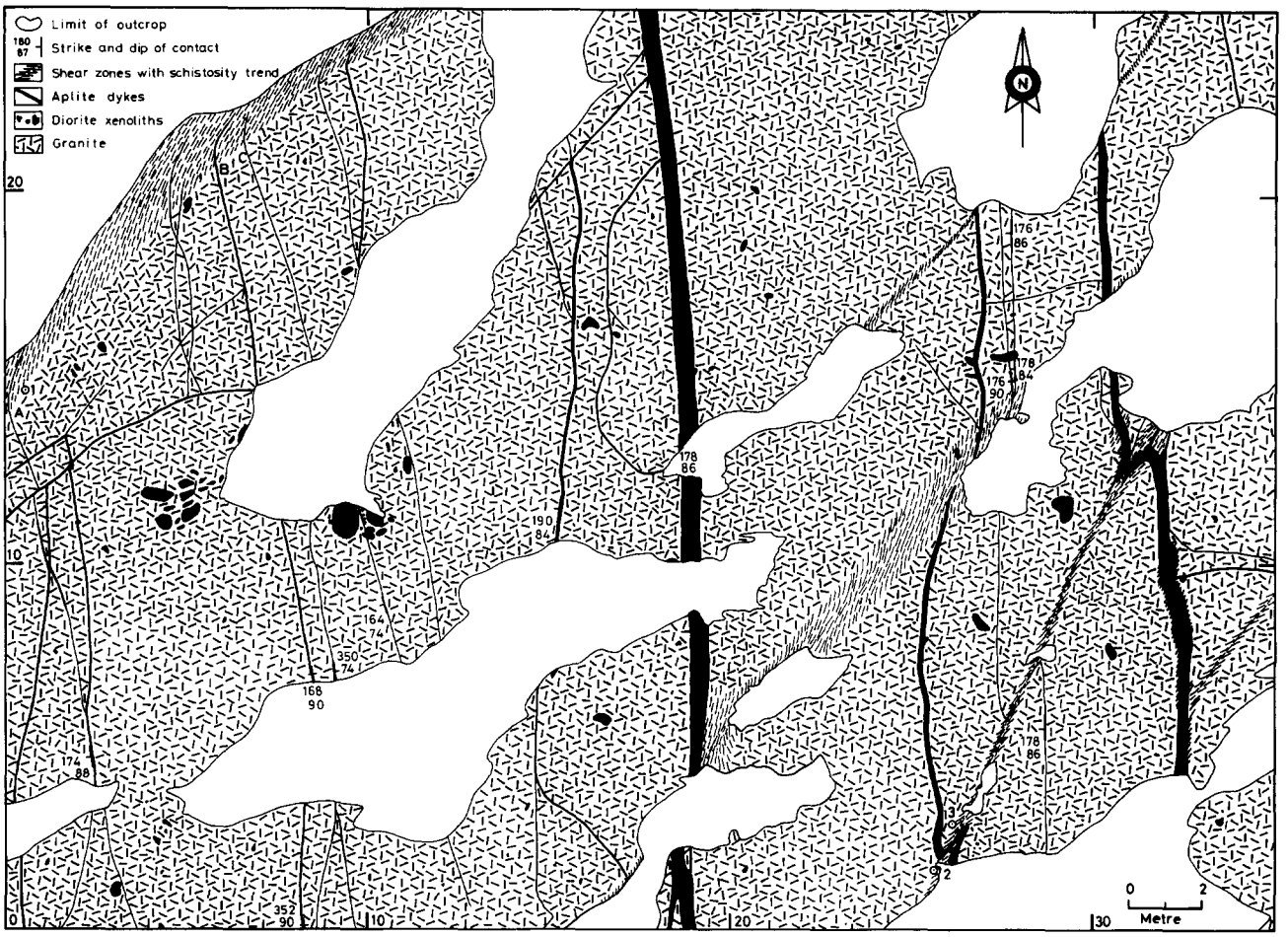

Fig. 4. Geological map of the studied area.

fig. 18). Considering this curved aspect, we have used one planar marker and the orientation of schistosity near it for strain determination. Uneven nature of the ground in the western part of the area did not permit us to map both boundaries of the shear zone. However, when traced towards the southwestern corner, both boundaries of the shear zone were found to be parallel. This parallelism is also supported by identical strain profiles of the shear zone at different locations. The orientations of dykes and schistosity inside shear zones were measured in pairs equidistant from the shear zone boundary, and the orientations of the dykes outside the shear zone were also measured (see the Appendix). The undeformed nature of the wall rocks allows us to apply the boundary condition of deformation by simple shear and volume loss. The results of these analyses are shown in the Appendix and Fig. 6. Both the shear strain and volume loss show systematic increase towards the centre of the shear zone, and they have a non-linear relation with each other (Fig. 7a). Since simple shear is a mechanism of deformation that conserves volume, the volume loss (Δ) is an independent variable in the diagram. On the other hand, the amount of shear strain (γ) is dependent on the volume factor (see equation 5). The curves are asymptotic towards the Δ axis, indicating that the shear strain increases more rapidly than volume loss, with progressive deformation. The ellipticity (R) of the finite strain ellipse, calculated from each pair of shear strain and volume loss factors, also shows a similar pattern, but increases at a more rapid rate than the shear strain (Fig. 7b). In both the cases, the strain paths resemble typical steady-state processes. The possible significance of this aspect will be discussed in a later section.

It can be seen from this analysis that the formation of ductile shear zones in the Maggia nappe involved a remarkably high amount of volume loss (nearly 90%) at their centres. The strongly heterogeneous nature of deformation, resulting in a non-linear distribution of volume loss, prevents us determining any average value from the analysis. Initially, this amount of volume change was thought to be excessive and we therefore analysed the amount of error from different sources that could have contributed to such a high value of volume loss.

Possible sources of error

The method of strain partitioning discussed above is based on angular measurements. Considering the fact that any error in measurement could be a possible source of error in the result, particularly where the angular differences are small, the actual data were changed by $\pm 2°$ and reanalysed to see the difference in the calculations. The results indicate that the errors are negligible until the amount of shear strain (γ) reaches a value of nearly 1. Even at low shear strains ($\gamma \leq 1$) the amount of calculated volume loss reaches values as high as 30–40%. At high shear strains, the following results were obtained.

(1) A $\pm$ 2° error in the measurement of dyke orientation outside the shear zone does not change the value of volume loss, but it does change the calculated value of shear strain by very small amounts.

(2) A $\pm$ 2° error in the measurement of dyke orientation inside the shear zone does not significantly affect volume loss, but it can give rise to large errors in the calculated value of shear strain.

(3) A $\pm$ 2° error in the measurement of schistosity orientation changes the amount of volume loss by $\pm$ 10%, and the amount of shear strain by $\pm$20%.

(4) A decrease in the angle between the dyke inside the shear zone and the shear direction, has the opposite effect to that of a decrease in the angle between the schistosity and the shear direction (Fig. 8).

A second possible source of error could arise if the observation surface is not a true profile. As can be seen from the map, the dykes mapped in the area are mostly vertical or nearly so. At a few places where cross joints allow measurement, the schistosity orientations were measured; these are vertical. Since the schistosity trend at the shear zone boundary makes an angle of 45° with the shear zone boundary, we assume the direction of shear movement to lie in the plane of measurement, or at least at a very low angle to it. Where the measurement surface is not exactly the profile plane, but is at a low angle to it, the angular relations of the surfaces which are vertical will not change; only the angular relations of subvertical surfaces will change slightly. This only results in small errors with values similar to those discussed earlier.

A third source of error could arise if the dykes are non-planar. We have mentioned earlier that only planar dykes were used for the analysis. Furthermore, as discussed above, a slight change in dyke orientation would not affect the amount of volume loss very much.

Considering these possible errors, where the computed mean volume loss is greater than 40%, there could be an error of $\pm$10% at any locality. Therefore, we were satisfied with the overall accuracy of deductions made from the geometrical features and we decided to look at the mineralogy and chemistry of the rocks from the shear zones and their immediate wall rocks of the region.

THE PROBLEM OF VOLUME LOSS

During the last two decades, numerous modal and chemical analyses of rocks from shear zones and outside shear zones have been presented from different parts of the world. For example, Beach (1976) has shown that granulite facies rocks of the Lewisian complex of Scotland show considerable change in mineralogy and composition inside shear zones, and the amount of change is closely related to the intensity of deformation. Mitra (1978) studied mineralogical variation in ductile shear zones in the Precambrian basement rocks of Blue Ridge region of Virginia, and showed that quartz monzonites (an essentially feldspar-rich rock) changes to a mica-rich

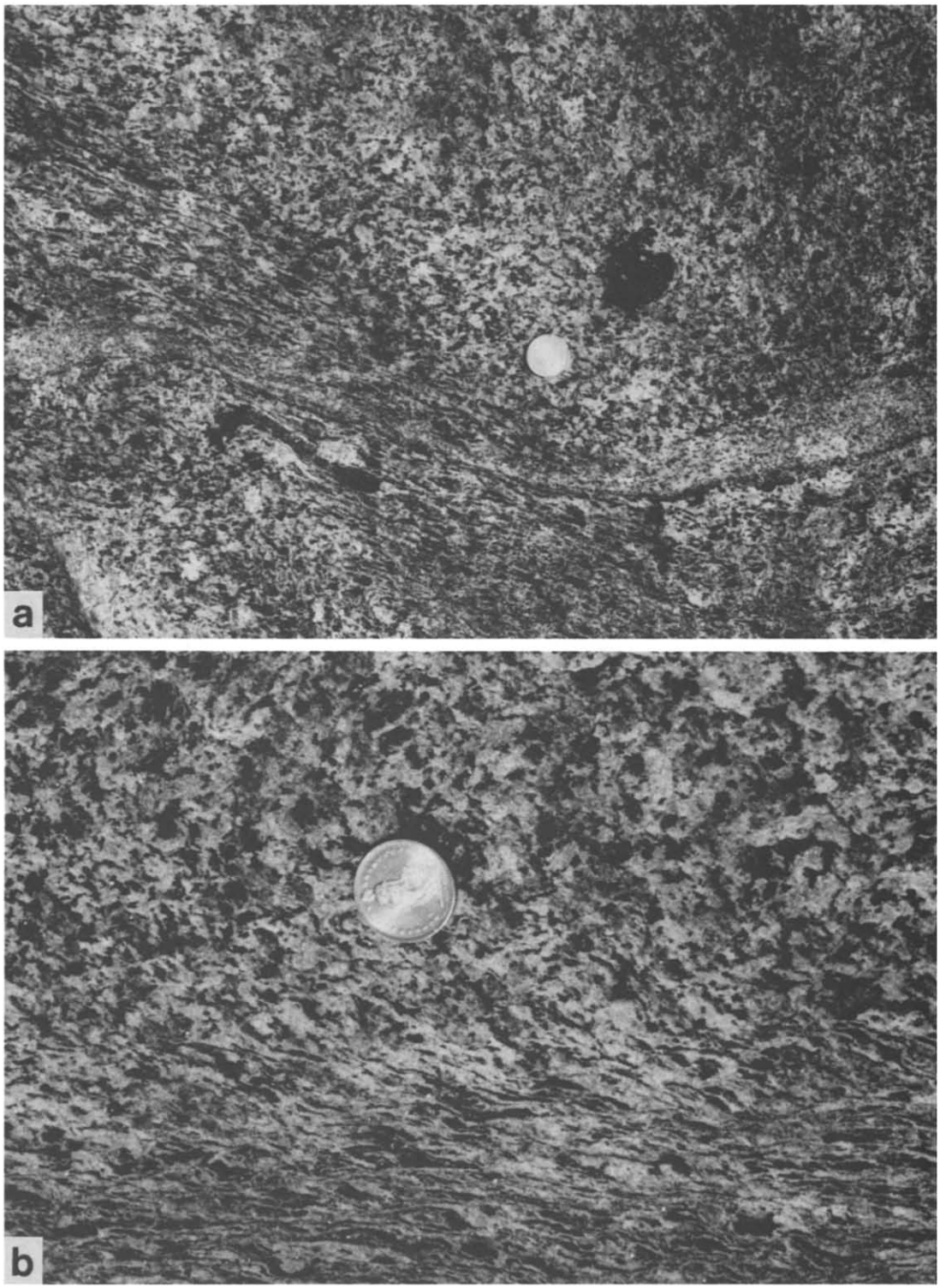

Fig. 5. (a) A ductile shear zone with undeformed walls, deflected marker, sigmoidal schistosity and deformed xenolith. (b) Detailed pattern of fabric in a shear zone and its wall.

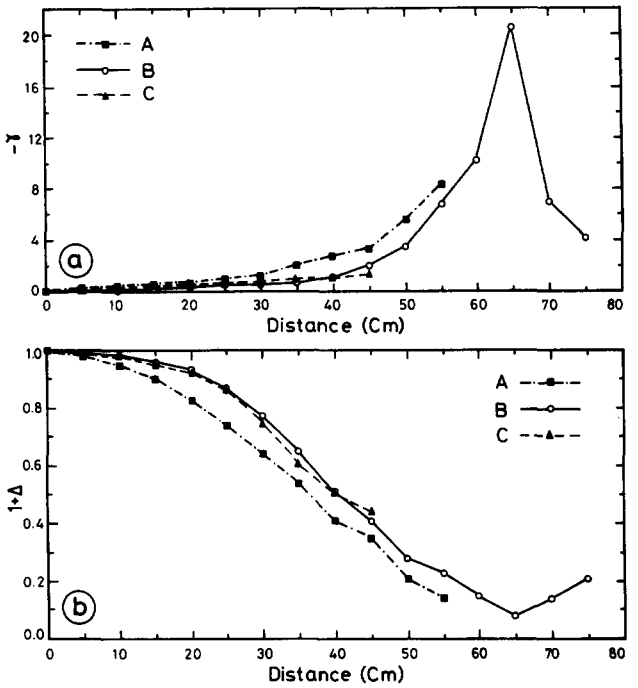

Fig. 6. Strain profiles of the analysed shear zone. (a) Variation in shear strain from shear zone boundary (distance = 0). (b) Variation in volume loss factor from shear zone boundary.

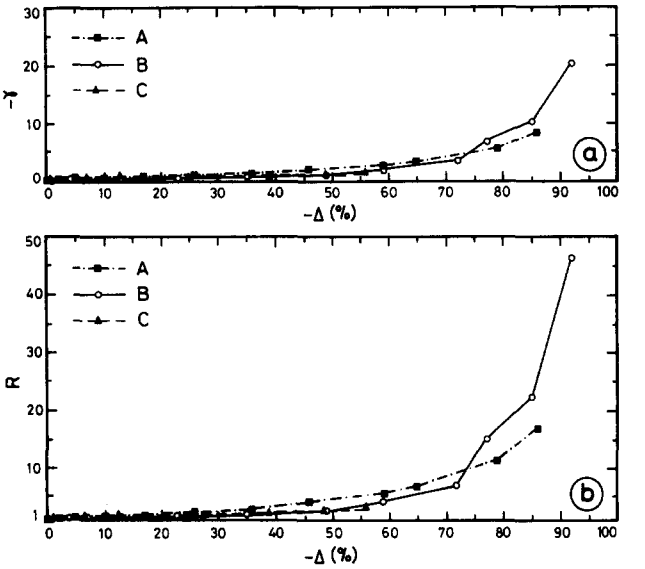

Fig. 7. Relationship between volume loss and (a) shear strain, and (b) ellipticity of strain ellipse in the studied area.

rock inside the shear zones. Most of the other studies, though convincingly demonstrating a close relation between the mineralogical and chemical changes in rocks and the intensity of deformation in shear zones, attribute such changes only to syn-kinematic metasomatic changes due to passage of large volume of fluids through the shear zone; the possible amount of volume change that could have taken place during such metasomatic changes is rarely discussed.

Analyses of chemical composition–volume relations of samples collected from undeformed wall and progressively more deformed parts of small-scale shear zones from the Laghetti area (see Fig. 3c for sample locations and Table 1 for data) in the light of a method outlined by Gresens (1967), led Kerrich *et al.* (1977) and Simpson (1981, 1983) to conclude that the shear zones of this region developed without significant volume change. These conclusions were based on identical results obtained with first an assumption of no volume change, and second with an assumption of immobility of Al_2O_3. If we assume that both the content of Al_2O_3 and the volume of rock inside shear zones of the Laghetti area could vary, and that the loss or gain of Al_2O_3 took place at the same rate at which the volume was changed, the results obtained from calculations assuming no volume change and immobility of Al_2O_3 will be similar. Therefore, the results obtained by the two assumptions used by Kerrich *et al.* (1977) and Simpson (1981, 1983)

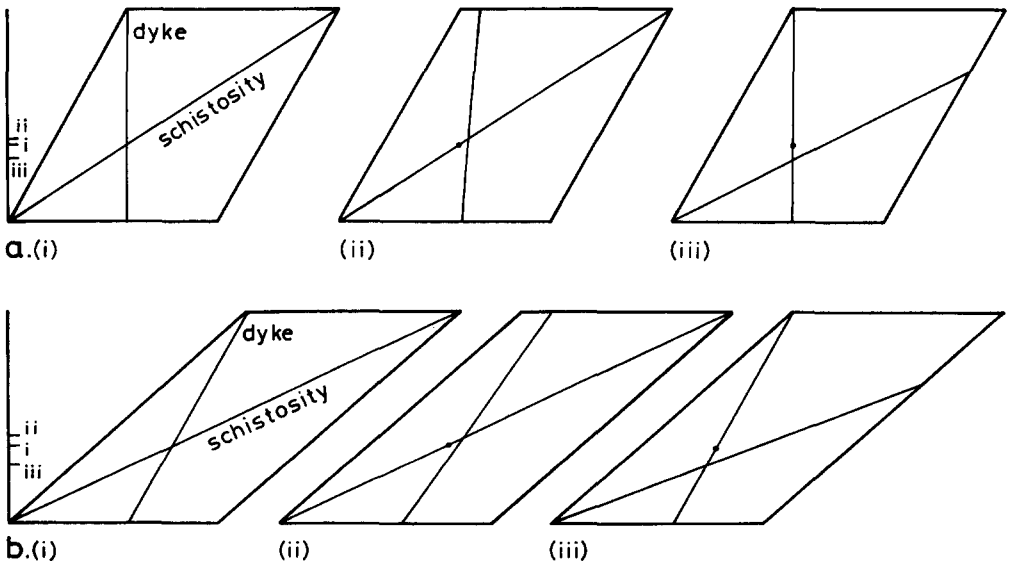

Fig. 8. Schematic diagrams showing the effects of errors in measurement (a) at low strain and (b) at high strain. (i) Correct orientation, (ii) dyke orientation changed by −5°, and (iii) schistosity orientation changed by −5°. The position of the point of intersection between the dyke and schistosity for the correct orientations is marked by a dot in (ii) and (iii), and the relative changes in the volume loss factor are shown in (i).

Table 1. Major-element composition of rocks (in wt %) from three shear zones in the Maggia nappe (source of data: Simpson 1981)

Locality*	S1			S2			S3	
Sample number†	G110 (A)	G107 (B)	G109 (C)	G25 (A)	G27 (B)	G28 (C)	D15 (A)	D32 (C)
SiO_2	56.89	60.75	59.00	68.49	69.28	66.19	50.30	50.17
TiO_2	0.85	0.74	0.76	0.40	0.39	0.44	1.15	1.11
Al_2O_3	17.58	17.25	16.53	15.40	14.96	16.67	18.14	16.00
Fe_2O_3 (Fe_t)	7.09	5.67	6.78	3.57	3.36	3.85	9.85	10.20
MnO	0.13	0.09	0.12	0.08	0.08	0.09	0.15	0.15
MgO	3.14	2.56	3.26	0.98	0.99	1.10	5.48	7.99
CaO	6.27	4.89	5.81	3.07	2.88	3.55	8.26	9.53
Na_2O	2.85	3.40	2.26	3.40	3.35	3.36	2.05	1.82
K_2O	2.83	2.61	2.82	3.12	3.64	3.35	2.49	1.15
P_2O_5	0.21	0.20	0.18	0.13	0.13	0.14	0.18	0.11
H_2O^+	1.50	1.20	1.70	0.80	0.70	0.90	1.60	1.30
Total	99.34	99.36	99.22	99.44	99.76	99.64	99.65	99.53

*S1 = granodiorite, S2 = granite, S3 = tonalite (see Fig. 3c for sample location).
†A = undeformed, B = shear zone boundary, C = sheared rock.

Table 2. Modal composition of rocks (in volume %) from the Laghetti area

Minerals	Specimen No.* 1/*a*	1/*b*	2/*a*	2/*b*	3/*a*	3/*b*
Quartz	31.7	34.9	30.3	28.0	28.7	22.0
Plagioclase	26.7	30.0	36.3	44.3	41.0	45.2
K-feldspar	20.7	5.2	16.1	7.5	13.3	9.7
Biotite	14.5	17.8	14.2	16.5	13.0	17.0
Epidote	4.6	3.9	2.5	3.2	3.3	5.2
Muscovite	1.6	8.0	0.4	0.3	0.3	0.6
Others	0.2	0.0	0.0	0.0	0.2	0.0
Total†	100.0	99.8	99.8	99.8	99.8	99.7

*For each specimen *b* is more deformed than *a*.
†Based on 2000 counts.

are not independent of each other. The 'Gresens method' can be interpreted in an infinite number of ways, and Gresens suggested that a grouping of elements which plot close to each other should be examined together before drawing any valid conclusion. Kerrich *et al.* (1977) and Simpson (1981) assumed only Al_2O_3 to be immobile to draw their conclusions. The assumption for immobility of Al_2O_3 is probably not valid for the shear zones of Laghetti, for the reasons discussed below.

Study of mineralogical variation was carried out on samples showing a progressive change in the intensity of deformation (see Fig. 4 for sample locations). Thin sections etched by $BaCl_2$ and amaranth solutions, following the method outlined by Norman (1974), enable distinctions to be made between K-feldspar, plagioclase and quartz. Modal analyses indicate that the shear zones of the Laghetti area show progressive enrichment in biotite and depletion in K-feldspar from low-strain regions to high-strain regions (Table 2). As the solubility of K-feldspar is greater than that of mica (biotite), removal of some of the K-feldspar by solution led to an enrichment in biotite. This process is likely to result in loss of Al_2O_3 from the system, and therefore the assumption of immobility of Al_2O_3 in this area is open to question. On the other hand, because of the low solubility of biotite, it is reasonable to assume that Fe_t, Mg and Ti were less mobile than Al. This assumption is also supported by the analysis of component ratios (Table 3).

In all samples, the proportion of Ti with respect to the total content of both Fe_t, Mg and Ti, and Fe_t, Mg, Ti and Al, remains fairly constant. Except for the samples from locality S3, all samples show a negligible variation in the proportions of Fe_t and Mg in the total content of Fe_t, Mg and Ti (the maximum difference for each element is 3%), and this variation is random in nature. When Al is considered with Fe_t, Mg and Ti, the proportions of Mg and Ti are found to be constant, but the proportions of Fe_t and Al show considerable variation (the maximum difference is 6% for Al) and, at least in the samples analysed by Kerrich *et al.* (1977), there is a progressive loss of Al content with increasing deformation of the rocks. This further undermines the assumption of immobility of Al made by Kerrich *et al.* (1977). The only locality for which the content of Al remains unchanged, together with Fe_t, Mg and Ti, is S2. The samples from S3 show a considerable change in the proportion of Fe_t and Mg in the content of Fe_t, Mg and Ti (the maximum difference is 8% for Mg), but in the total content of Fe_t, Mg, Ti and Al, the proportions of Fe_t and Ti are constant, and the proportion of Mg increases by 7% and that of Al decreases by 7%.

For the reasons mentioned above, the data from Kerrich *et al.* (1977) and Simpson (1981) were recalculated using a 'standard cell', as explained by Barth (1948), and plotted in the composition–volume diagram of Gresens (1967). This was cross checked by a slightly modified version of the 'Gresens method' suggested by Potdevin & Marquer (1987). In the absence of density data for the samples analysed by Simpson (1981), the data were calculated assuming the density ratio of the samples under comparison to be 1. This is reasonable on

Table 3. Ratio of different elements in the samples analysed from the Maggia nappe. Samples K from Kerrich *et al.* (1977) and S from Simpson (1981)

	K					S1			S2			S3	
Elements	A	B	C	D	E	A	B	C	A	B	C	A	C
Fe/(Fe+Mg+Ti)	0.70	0.69	0.72	0.70	0.71	0.64	0.63	0.63	0.72	0.71	0.72	0.60	0.53
Mg/(Fe+Mg+Ti)	0.21	0.22	0.19	0.21	0.20	0.28	0.29	0.30	0.20	0.21	0.20	0.33	0.41
Ti/(Fe+Mg+Ti)	0.09	0.09	0.09	0.09	0.09	0.08	0.08	0.07	0.08	0.08	0.08	0.07	0.06
Fe/(Fe+Mg+Ti+Al)	0.19	0.19	0.21	0.20	0.24	0.25	0.21	0.25	0.17	0.17	0.17	0.29	0.29
Mg/(Fe+Mg+Ti+Al)	0.06	0.06	0.05	0.06	0.06	0.11	0.10	0.12	0.05	0.05	0.05	0.16	0.23
Ti/(Fe+Mg+Ti+Al)	0.02	0.03	0.03	0.03	0.03	0.03	0.03	0.03	0.02	0.02	0.02	0.03	0.03
Al/(Fe+Mg+Ti+Al)	0.73	0.72	0.71	0.71	0.67	0.61	0.66	0.60	0.76	0.76	0.76	0.52	0.45

the basis of the fact that density does not show any significant change in the samples analysed by Kerrich *et al.* (1977) from the same region, and thus the density ratio of any two samples is close to 1. The intercepts at the volume axis for no mass change of each element were calculated for assumptions of immobility of different elements. The average volume loss for no mass change of Fe_t, Mg and Ti was determined from these results. We also calculated the amount of volume loss assuming immobility of Fe_t, Mg, Ti and Al. The results of these calculations are shown in Table 4. Both these results strongly suggest that the development of the shear zones at Laghetti was involved with significant volume loss. It should be noted that the values given in Table 4 are estimates made on the basis of the assumption that the mass of the elements assumed to be less mobile did not change. If some amount of these components were also removed by solution in the same ratio, then the amount of volume loss would be higher than that given in the table. The contention that the supposed less mobile elements were removed by solution along with other more mobile elements can be seen from Table 4(b). The sample, S1-B, collected from the shear zone boundary shows significant increase in volume when compared with the undeformed wall, on the assumption of no mass change. If it is assumed that no significant volume change took place between the undeformed wall and the shear zone boundary, the result would imply a mass loss of about 20%. If this 20% mass loss had indeed taken place inside the shear zone, the amount of volume loss inside the shear zone would increase by nearly 20% over that estimated in Table 4(b).

The results obtained from the geometrical analysis and the chemical analyses are best interpreted in terms of volume loss in the shear zones of Laghetti. The most striking feature of these results is the very large amount of volume loss towards the centre of the shear zone, reaching a maximum of 92%. Such large volume losses has been reported only from a few places. Alternative models have been invoked in some instances to explain similar strain patterns to those seen at Laghetti. Schwerdtner (1982) described apparent volume losses from 48 to 68% in some natural deformation zones in the Grenville Front tectonic zone, Ontario. He suggested that volume losses of more than 30% are unrealistic but did not give reasons why they are unrealistic. Subsequently, Mawer (1983) analysed the state of strain in mylonite zones in the Chewing Range Quartzite of Central Australia, and obtained volume losses varying from 69% in the least deformed mylonite to nearly 95% in the most strongly deformed rocks, with most values between 83 and 95%. Mawer (1983), like Schwerdtner (1982), thought such a high volume loss to be unrealistic, and suggested that the observed strain pattern can be due to severe bulk shortening normal to the zones, without volume loss. However, such a model is geometrically incompatible with the shear zone geometry observed at Laghetti where successive profile sections along the shear zone are geometrically identical. Bulk shortening is a viable factor only where it occurs within the zone and identically within the shear zone walls, or where there are displacement differences by heterogeneous faulting in the zone (Ramsay & Huber 1987, pp. 611–613). Bell & Cuff (1989) reviewed the problem of volume loss and suggested that large amounts of volume loss can take place at all metamorphic grades.

FURTHER EVIDENCE IN FAVOUR OF HIGH VOLUME LOSS

Simpson (1981) carried out analyses of deformed xenoliths and shape changes of mineral aggregates in the shear zones of the Laghetti area. Most of the data plot

Table 4. Volume change (Δ) between different samples analysed from the Maggia nappe

(a) Source of chemical analysis data: Kerrich *et al.* (1977)

Locality	Samples*	Δ (assuming Fe_t, Mg and Ti to be immobile)	Δ (assuming Fe_t, Mg, Ti and Al to be immobile)
K	A–B	−2.8%	−1.6%
	A–C	−6.2%	−5.2%
	A–D	−10.1%	−8.1%
	A–E	−22.7%	−17.5%

(b) Source of chemical analysis data: Simpson (1981)

Locality	Samples†	Δ (assuming Fe_t, Mg and Ti to be immobile)	Δ (assuming Fe_t, Mg, Ti and Al to be immobile)
S1	A–B	+22.3%	+17.6%
	A–C	+4.7%	+5.3%
	B–C	−14.2%	−9.6%
S2	A–B	+1.6%	+3.2%
	A–C	−10.0%	−9.5%
	B–C	−11.4%	−11.2%
S3	A–C	−10.8%	−5.0%

*Sample A—collected from undeformed wall; samples B–E—progressively more deformed rock

†Sample A—collected from undeformed wall; sample B—collected from shear zone boundary; sample C—collected from shear zone centre.

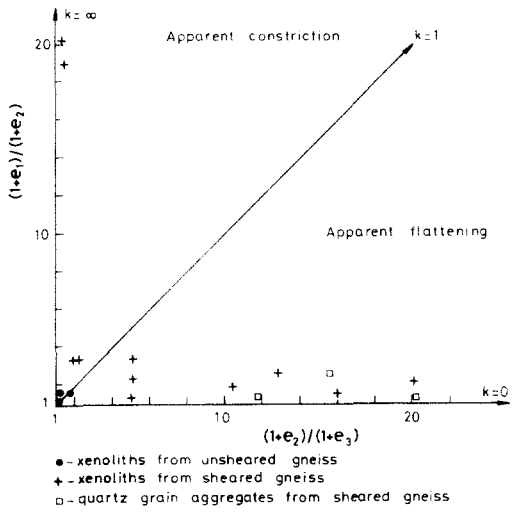

Fig. 9. Flinn diagram for deformed xenoliths and quartz grain aggregates from the Laghetti area (from Simpson 1981).

within the field of apparent flattening (Fig. 9). Since Simpson (1981, 1983) assumed no volume loss during deformation, from the results of chemical analyses, these strain patterns were interpreted to be the result of overprinting of an initial deformation by a later straining phase. However, for the interpretation of the fabric diagrams Simpson (1981, 1983) did not fully discuss the effect of this supposed later deformation. We maintain that plots of the axial ratios of the apparently flattened xenoliths and mineral aggregates from the shear zones of Laghetti, from compatibility constraints, cannot be due to subsequent deformation, but must be the result of volume loss. The amount of volume loss was calculated from Fig. 9, assuming plane strain, using the equation

$$\Delta = \frac{(1 + e_1)/(1 + e_2)}{(1 + e_2)/(1 + e_3)} - 1, \qquad (17)$$

where $1 + e_1$, $1 + e_2$ and $1 + e_3$ represent lengths of the semi-axes of ellipsoidal markers. The results indicate a maximum volume loss of nearly 90%, with most of the values clustered around 85%. Since this closely matches the results obtained independently by geometrical analysis of dykes and schistosity orientations from the same region, we feel justified in concluding that the formation of ductile shear zones in the Maggia nappe was by simple shear and volume loss; the latter reaching a maximum value of 80–90% towards the centres of some shear zones.

STRAIN PATH OF THE SHEAR ZONES IN THE MAGGIA NAPPE

Theoretical strain paths (Flinn 1962, 1978, Elliott 1972, Ramsay & Wood 1973, Ramberg 1975) were computed for constant volumetric and shear strain increments with the same boundary conditions as outlined for ductile shear zones with undeformed walls (see equation 5; see also Ramsay & Huber 1983, pp. 217–234, for the method of calculation). The amount of finite volume loss

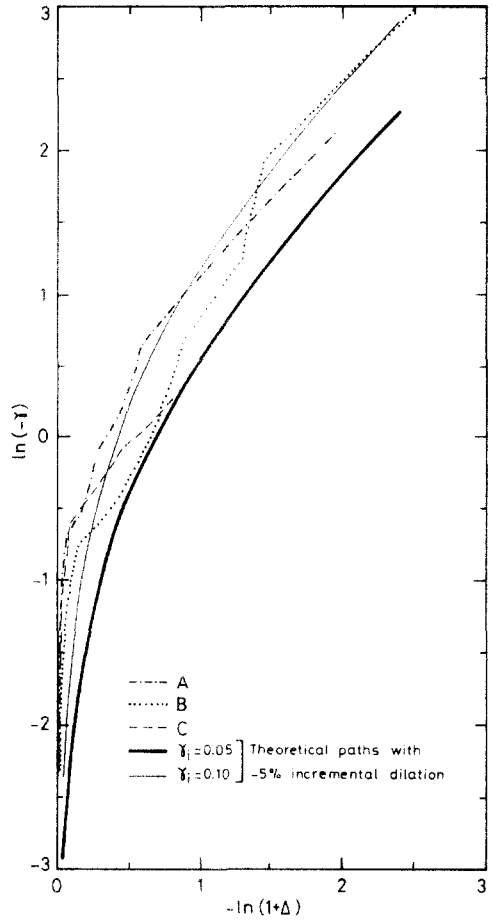

Fig. 10. Strain path of a shear zone from the Laghetti area.

clearly only depends on the rate of dilation and is independent of the shear strain rate. We decided to investigate possible links between the total volume change and total shear and to see how these features might be interpreted in terms of incremental strain geometry of both factors. To do this we calculated finite dilation-shear strain values for steady-state increments in which the proportion of incremental dilation (Δ_i) to incremental shear strain (γ_i) remains constant. After the end of each increment, dilation and shear strain values were computed from the strain matrix by using equation (5). The values of finite dilation and finite shear strain accumulate in a non-linear fashion (Fig. 10): a well known feature of practically all types of steady-state incremental deformation (Ramsay & Huber 1983, pp. 22 and 222). Curves with a higher proportion of incremental shear relative to incremental dilation lie above those with a lower proportion of these two factors.

The strain data computed from field observations were compared with the theoretical strain paths (Fig. 10). At low-strain conditions, the paths for natural data lie above the computed curves, then cross them, indicating non-steady-state deformation. However, at high strains the paths of natural data closely follow those of the theoretical paths, suggesting steady-state processes linking the proportion of volumetric incremental change (Δ_i) to that of incremental shear strain (γ_i). At low strain the path is close to one of incremental deformation of 1–

3% volume loss with 0.05–0.1γ, and at high strain, the path is close to that of incremental deformation of 5% volume loss with 0.05–0.1γ. This implies that if the shear strain rate remained constant during deformation, the rate of volume loss progressively increased until a volume reduction of 5% was achieved. Above this value the proportion of volume change is linked to the proportion of shear strain. This is probably best attributed to the fact that grain-size reduction at early stages of deformation increased the porosity of the rock (leading to increasing solution-transfer of materials) but after a stage when the grain-size reached a critical steady state value, no further increase in porosity (and solution-transfer) could take place. These results also imply that, if volume loss was continually taking place (neglecting the lower value at an early stage of deformation), it would be possible to reach a volume loss of 90% with a shear strain value of γ approximately 20.

SUMMARY AND CONCLUSIONS

Ductile shear zones in Hercynian granite intrusions in basement gneisses at the core of the Maggia nappe, were developed by heterogeneous simple shear and volume change during early and main deformation phases of Alpine orogeny. Partitioning of different components of strain by geometrical analyses using planar markers inside and outside a shear zone and schistosity inside the shear zone, shows a good correlation between shear strain and volume loss. The amount of volume loss, reaching a maximum of 80–90%, although rather high, is also supported from finite strain data from the same region. Changes in whole rock chemical and mineralogical composition also suggest volume loss. The undeformed nature of the wall rocks and the orientations of schistosity inside the shear zones preclude the possibility of the observed strain pattern being the result of subsequent deformation. Analysis of the strain path of the shear zones of the area indicates that the shear strain remained constant during deformation, but that the rate of dilation gradually increased during the early stage, probably due to grain-size reduction resulting in increasing porosity, and remained constant during late stages of deformation.

Acknowledgements—The authors are thankful to OFIMA, Locarno, for providing accommodation in the field, and to Peter Berchtold, Alain Hohl, Michael Rüffer, and Thomas Stoll, of the Mineralogie–Petrographie Institut, ETH-Zürich, for logistic support during fieldwork. Professor A. B. Thompson offered constructive suggestions about the 'Gresens method', but the interpretations are the full responsibility of the authors. S. Mohanty is grateful to the Ministry of Human Resource Development, Government of India, for a postdoctoral scholarship.

REFERENCES

Ayrton, S. N. & Ramsay, J. G. 1974. Tectonic and metamorphic events in the Alps. *Schweiz. miner. petrogr. Mitt.* **54**, 609–639.

Barth, T. F. W. 1948. Oxygen in rocks: a basis for petrographic calculations. *J. Geol.* **56**, 50–60.

Beach, A. 1976. The interrelations of fluid transport, deformation, geochemistry and heat flow in early Proterozoic shear zones in the Lewisian complex. *Phil. Trans. R. Soc. Lond.* **A280**, 569–604.

Bell, T. H. & Cuff, C. 1989. Dissolution, solution transfer, diffusion versus fluid flow and volume loss during deformation/metamorphism. *J. metamorph. Geol.* **7**, 425–447.

Elliott, D. 1972. Deformation paths in structural geology. *Bull. geol. Soc. Am.* **83**, 2621–2638.

Flinn, D. 1962. On folding during three-dimensional progressive deformation. *Q. J. geol. Soc. Lond.* **118**, 385–433.

Flinn, D. 1978. Construction and computation of three-dimensional progressive deformations. *J. geol. Soc. Lond.* **135**, 291–305.

Gratier, J. P. 1983. Estimation of volume changes by comparative chemical analyses in heterogeneously deformed rocks (folds with mass transfer). *J. Struct. Geol.* **5**, 329–339.

Gresens, R. L. 1967. Composition-volume relationships of metasomatism. *Chem. Geol.* **2**, 47–65.

Huber, M., Ramsay, J. G. & Simpson, C. 1980. Deformation in the Maggia and Antigorio nappes, Lepontine Alps. *Eclog. geol. Helv.* **73**, 593–606.

Kerrich, R., Fyfe, W. S., Gorman, B. E. & Allison, I. 1977. Local modification of rock chemistry by deformation. *Contr. Miner. Petrol.* **65**, 183–190.

Klaper, E. M. 1982. Deformation und Metamorphose in der nördlichen Maggia-zone. *Schweiz. miner. petrogr. Mitt.* **62**, 47–76.

Köppel, V., Günthert, A. & Grünenfelder, M. 1981. Patterns of U–Pb zircon and monazite ages in polymetamorphic units of the Swiss Central Alps. *Schweiz. miner. petrogr. Mitt.* **61**, 97–119.

Mawer, C. K. 1983. State of strain in quartzite mylonite, Central Australia. *J. Struct. Geol.* **5**, 401–409.

Mitra, G. 1978. Ductile deformation zones and mylonites: the mechanical processes involved in the deformation of crystalline basement rocks. *Am. J. Sci.* **278**, 1057–1084.

Norman, M. B. II. 1974. Improved technique for selective staining of feldspar and other minerals using amaranth. *J. Res. U.S. geol. Surv.* **2**, 73–79.

Potdevin, J.-L. & Marquer, D. 1987. Quantitative methods for the estimation of mass transfers by fluids in deformed metamorphic rocks. *Geodinamica Acta* **1**, 193–206.

Ramberg, H. 1975. Particle paths, displacement and progressive strain applicable to rocks. *Tectonophysics* **28**, 1–37.

Ramsay, J. G. 1980. Shear zone geometry: a review. *J. Struct. Geol.* **2**, 83–99.

Ramsay, J. G. & Allison, I. 1979. Structural analysis of shear zones in an alpinised Hercynian granite (Maggia Nappen, Pennine zone, central Alps). *Schweiz. miner. petrogr. Mitt.* **59**, 251–279.

Ramsay, J. G. & Graham, R. H. 1970. Strain variation in shear belts. *Can. J. Earth Sci.* **7**, 786–813.

Ramsay, J. G. & Huber, M. I. 1983. *The Techniques of Modern Structural Geology, Volume* 1: *Strain Analysis*. Academic Press, London.

Ramsay, J. G. & Huber, M. I. 1987. *The Techniques of Modern Structural Geology, Volume* 2: *Folds and Fractures*. Academic Press, London.

Ramsay, J. G. & Wood, D. S. 1973. The geometric effects of volume change during deformation processes. *Tectonophysics* **16**, 263–277.

Schwerdtner, W. M. 1982. Calculation of volume change in ductile band structures. *J. Struct. Geol.* **4**, 57–62.

Simpson, C. 1981. Ductile shear zones: a mechanism of rock deformation in the orthogneisses of the Maggia Nappe, Ticino. Unpublished Ph.D. thesis, ETH-Zürich.

Simpson, C. 1983. Strain and shape-fabric variations associated with ductile shear zones. *J. Struct. Geol.* **5**, 61–72.

APPENDIX

Table A1. Measurements of planar structures from a shear zone with respect to the shear zone boundary, and separation of strain factors

Locality	Distance (cm)	Orientation of dyke (°)	Orientation of schistosity (θ'',°)	Shear strain (γ)	Volume factor ($1 + \Delta$)
A	0	$\alpha = 50$	—		
	5	$\alpha' = 44$	40	−0.18	0.98
	10	38	36	−0.40	0.95
	20	34	32	−0.55	0.90
	25	32	28	−0.59	0.83
	30	26	24	−0.92	0.74
	35	22	20	−1.17	0.64
	40	16	16	−1.93	0.54
	45	12	12	−2.67	0.41
	50	10	10	−3.26	0.35
	55	06	06	−5.54	0.21
	60	04	04	−8.36	0.14
B	0	$\alpha = 58$	—		
	5	$\alpha' = 54$	42	−0.10	0.99
	10	52	39	−0.14	0.98
	15	49	36	−0.22	0.96
	20	45	34	−0.33	0.93
	25	40	30	−0.47	0.87
	30	37	24	−0.52	0.77
	35	32	18	−0.64	0.65
	40	24	14	−1.03	0.51
	45	16	12	−1.96	0.41
	50	10	08	−3.40	0.28
	55	06	06	−6.81	0.23
	60	04	04	−10.27	0.15
	65	02	02	−20.58	0.08
	70	05	04	−6.94	0.14
	75	08	06	−4.13	0.21
C	0	$\alpha = 72$	—		
	5	$\alpha' = 66$	42	−0.12	0.99
	10	60	39	−0.25	0.98
	15	54	36	−0.39	0.95
	20	50	34	−0.49	0.93
	25	46	30	−0.59	0.87
	30	42	24	−0.68	0.75
	35	34	18	−0.95	0.61
	40	30	14	−1.09	0.51
	45	26	12	−1.31	0.44